

## SPECIAL PROJECT FINAL REPORT

All the following mandatory information needs to be provided.

<b>Project Title:</b>	Near-term Climate Prediction at High Resolution
<b>Computer Project Account:</b>	spesiccf
<b>Start Year - End Year :</b>	2020 - 2021
<b>Principal Investigator(s)</b>	Etienne Tourigny
<b>Affiliation/Address:</b>	Barcelona Supercomputing Center Plaça Eusebi Güell, 1-3 08034 Barcelona (Spain)
<b>Other Researchers (Name/Affiliation):</b>	Aude Carreric, Pablo Ortega, Miguel Castrillo, Pierre-Antoine Bretonnière, Eric Ferrer, Roberto Bilbao, Juan Acosta Navaro, Vladimir Lapin, Yohan Ruprich-Robert

## **Summary of project objectives**

The main objective of the first set of experiments (year 1) is to better understand the climate impacts of the observed AMV in order to estimate their predictability. This has been done by performing idealized experiments with EC-Earth3 CGCM in which the North Atlantic SST is restored towards the observed AMV anomalies. We particularly focus on the AMV impacts on the occurrence of weather extremes such as Tropical Cyclones, heat waves, and heavy precipitation events. In the second part (year 2), we explore the impact of increasing horizontal resolution on the oceanic and atmospheric domains on seasonal prediction skill of EC-Earth3 through retrospective seasonal predictions. Specific emphasis has been made on improvements in simulating North Atlantic climate variability, and how it affects simulated climate over land areas including Europe, and climate extremes.

## **Summary of problems encountered**

The covid-19 has had a strong negative impact on this project during the first year, and strong measures were put in place to deal with the situation. This had an impact on the SBU hours consumed in the first year of the project.

The first long simulations performed with the high-resolution (HR) version of EC-Earth3 used for the second part of this project, revealed an unrealistically cold climate over the North Atlantic sector, strong enough to degrade the skill of the forecasts. To reduce this bias and thus produce better forecasts, a retuning effort of this version of the model has been done during the first implementation period of the project.

## **Experience with the Special Project framework**

The only suggestion I would have is to delay by a few months the deadline to submit new applications. As it stands the deadline is in the middle of the calendar year which is quite a long time before the start of the next period. If we were given a few more months (if possible) our requests would more accurately reflect our needs for the following year.

## **Summary of results**

### Part 1 - Predictability of the impacts linked to the Atlantic Multidecadal Variability

The first part of the results summary is related to the impacts of the Atlantic Multidecadal Variability (AMV).

Idealized AMV experiments were performed with EC-Earth3P-HR, the high resolution (ORCA025L75-T511L91) HighResMIP version of EC-Earth (Haarsma et al., 2020). Following the DCP-C protocol (Boer et al. 2016), two sets of ensemble simulations have been conducted, in which time-invariant SST anomalies corresponding to the warm (AMV+) and cold (AMV-) phases of the observed AMV were imposed over the model North Atlantic using SST nudging. To capture the potential response and adjustment of other oceanic basins to the AMV anomalies, the simulations were integrated for 10 years with fixed external forcing conditions. Ensemble simulations of 17 members were performed in order to robustly estimate the climate impacts of the AMV (only 10 of them were performed on CCA). An extensive description of the experimental protocol is provided in the Technical note for AMV DCP-C simulations:

<https://www.wcrp-climate.org/wgsip/documents/Tech-Note-1.pdf>. Similar experiments with the standard resolution of EC-Earth3P (ORCA1L75-T255L91) were performed in another supercomputer (Marenostrum 4, BSC) and are used to explore the impacts of model resolution on our ability to capture the observed AMV teleconnections. For those standard resolution experiments we performed 25 ensemble members for both AM+ and AMV-.

Results from the EC-Earth3P and EC-Earth3P-HR experiments show overall very similar results in summer (Figure 1). In particular, in response to a North Atlantic warming of  $\sim 0.25^{\circ}\text{C}$  the models simulate a South Atlantic cooling ( $\sim -0.05^{\circ}\text{C}$ ) and a warming in the eastern Indian Ocean and the Maritime Continent ( $\sim 0.10^{\circ}\text{C}$ ; Figure 1ab). Over the Pacific, temperature anomalies project strongly onto the negative phase of the Inter-decadal Pacific Oscillation, with negative SST anomalies in the tropical Pacific that extend toward the pole in both hemispheres in a horseshoe-like pattern that surrounds positive SST anomalies in the west. Over land, models simulate warm anomalies over the Americas reaching up to  $0.25^{\circ}\text{C}$  as well as warming over the Mediterranean region and over the Eurasian continent.

In terms of sea level pressure (Figure 1cd), an AMV warming leads to low pressure anomalies over a large North Atlantic – Europe region, which is mass compensated by high pressure anomalies over the Pacific Ocean, indicating a modification of the Walker Circulation. This is confirmed by the precipitation anomalies (Figure 1ef) that reveal a northward shift of the Inter-Tropical Convergence Zone (ITCZ) over the Atlantic, the eastern Pacific and the Sahel. Negative precipitation anomalies prevail over the western and central tropical Pacific in both hemispheres, which corresponds to a southward tilt of the South Pacific Convergence Zone (SPCZ) and a southward shift of the ITCZ.

Over the extra-tropics, both models simulate a small but significant rainfall increase over the North Atlantic, consistently with the imposed SST warming that increases the evaporation and the amount of precipitable water. The two models also show drier conditions over South and North America in response to a North Atlantic warming, as well as precipitation increase over India, indicating an impact of AMV on the Asian monsoon. We note that the results from our experiments are consistent with the AMV impacts previously documented in the literature (e.g., Zhang and Delworth 2006; Dong et al. 2006; Zanchettin et al. 2016; Ruprich-Robert et al. 2017, 2018).

During winter, the climate responses to the imposed AMV are comparable between the two models and qualitatively similar to the summertime ones (Figure 2). However, we note a different response in terms of sea level pressure over the extra-tropical North Atlantic sector, with EC-Earth3P simulating negative anomalies centered East of Europe (Figure 2e) and EC-Earth3P-HR simulating positive anomalies centered over the subpolar gyre (Figure 2f). In the multi-model study of Ruggieri et al. (2021), which includes our EC-Earth3P AMV simulations, we investigated the difference of model responses to AMV forcing over this region in winter. We were able to link those different responses to the different model mean states. In particular, we showed that models simulating a more realistic northward excursion of the extra-tropical jet also simulate stronger wind decrease over the North Atlantic subpolar region in response to an AMV warming. This result indicates that mean model biases impact models ability to simulate climate responses to the observed AMV anomalies. Analysis is ongoing to evaluate whether the differences of sea level pressure responses over the North Atlantic between EC-Earth3P and EC-Earth3P-HR are consistent with the results of Ruggieri et al. (2021).

In addition, the amplitude of the central tropical Pacific cooling response to AMV warming is slightly different between our two model resolutions: the NIÑO3.4 SST cooling reaches  $-0.17^{\circ}\text{C}$  in EC-Earth3 and  $-0.12^{\circ}\text{C}$  in EC-Earth3P-HR. In Ruprich-Robert et al. (2021), we investigated the reasons leading to this different model response comparing 21 AMV simulations performed by 13 different models, including EC-Earth3P and EC-Earth3P-HR. We found that models differ by a factor 10 in simulating the amplitude of the Equatorial Pacific cooling response to observed AMV

warming. Using energy constraint approaches, we tracked back the origins of this spread. We found that the large inter-model spread is mainly driven by different amounts of moist static energy injection from the tropical Atlantic surface into the upper troposphere, which is mostly due to different models mean ITCZ positions and strengths. Analytically correcting models for their mean precipitation biases, we reduce this inter-model uncertainty and we quantify that, following an observed 0.26°C AMV warming, the equatorial Pacific cools by 0.11°C with an inter-model standard deviation of 0.03°C.

Overall, the analyses we conducted, including the idealized AMV experiments performed on the ECMWF supercomputer, point to different model representations of the observed AMV climate impacts due to different model mean states. Therefore, the differences seen between EC-Earth3P and EC-Earth3P-HR results cannot be attributed purely to a change of resolution only. To assess in a more robust way the effects of model resolution on the representation of the AMV impacts, we explored the systematic differences between sets of paired AMV experiments performed with the same model but at two different resolutions. For this specific analysis, we compared the results from for different models: CNRM-CM6-1/CNRM-CM6-1-HR, EC-Earth3/EC-Earth3P-HR, ECMWF-IFS/ECMWF-IFS-HR, MetUM-GOML2/MetUM-GOML2-HR and MPI-ESM1-2/MPI-ESM1-2-HR. Using an analysis of variance (ANOVA) to disentangle between the different sources of inter-model spread in the AMV responses, we found in Hodson et al. (2021, submitted to Climate Dynamics) that models responses are generally unchanged by increasing resolution except concerning the northward displacement of the ITCZ in response to an AMV warming, moving further north at higher resolution.

However, we acknowledge that so far we focused on the large-scale impacts of the AMV, for which we found that model mean state variations are likely the most significant source of uncertainty. Resolution may play a greater role for smaller scale processes or extremes, such as hurricanes or temperature extremes. Future studies will examine those impacts. Given the widespread nature of the impacts of the AMV seen in this report, a better understanding of these model uncertainties, combined with good estimates of the future evolution of the AMV are crucial to predict near-term global climate changes.

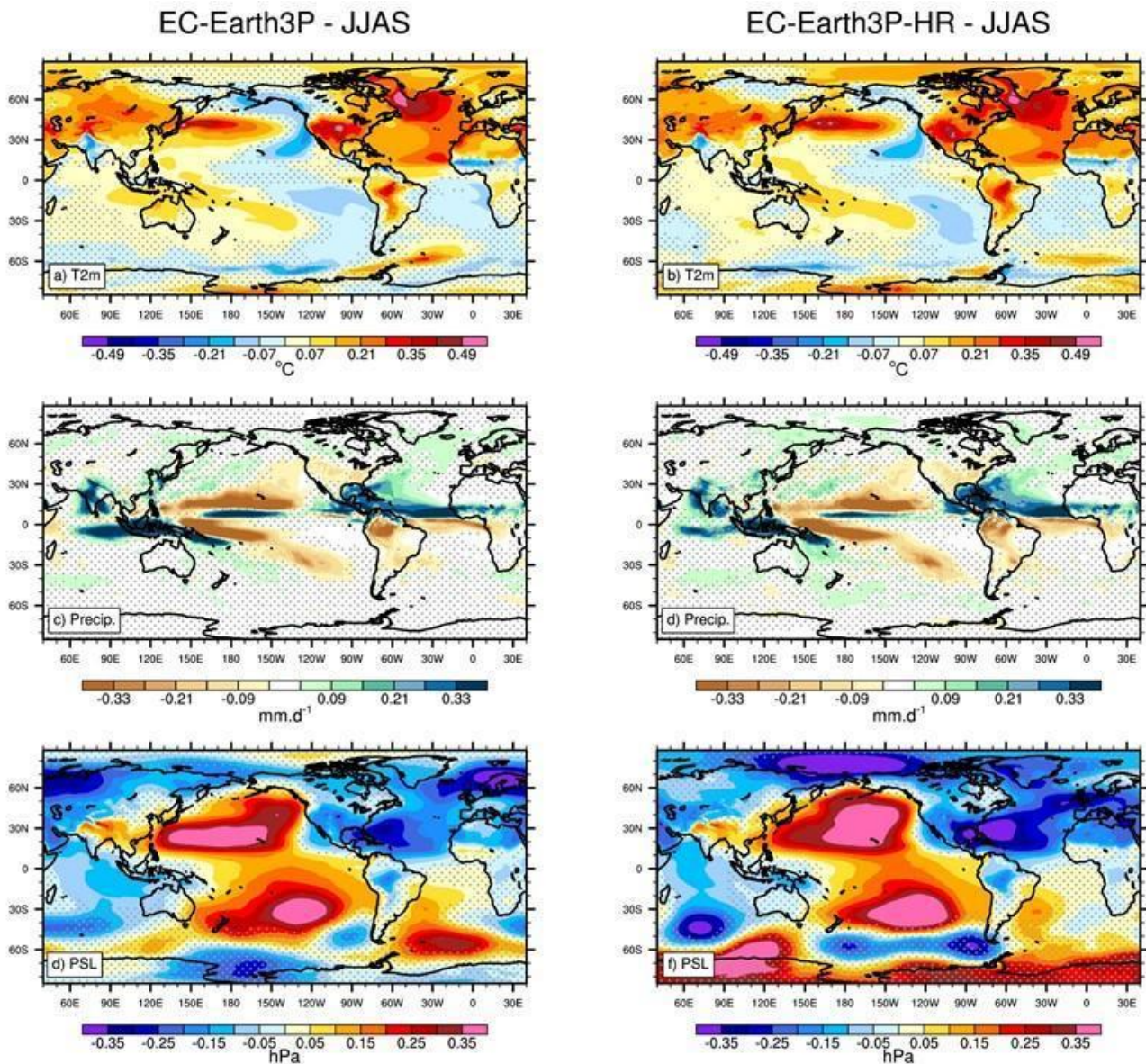


**Figure 1:** Differences between the 10-yr average of AMV+ and AMV- ensemble simulations for the JJAS season. (a), (b) 2-meter air temperature, (c), (d) precipitation, and (e), (f) sea level pressure. Results from (left) EC-Earth3 and (right) EC-Earth3P-HR are shown. Stippling indicates regions that are below the 95% confidence level of statistical significance according to a two-sided Student's t test.

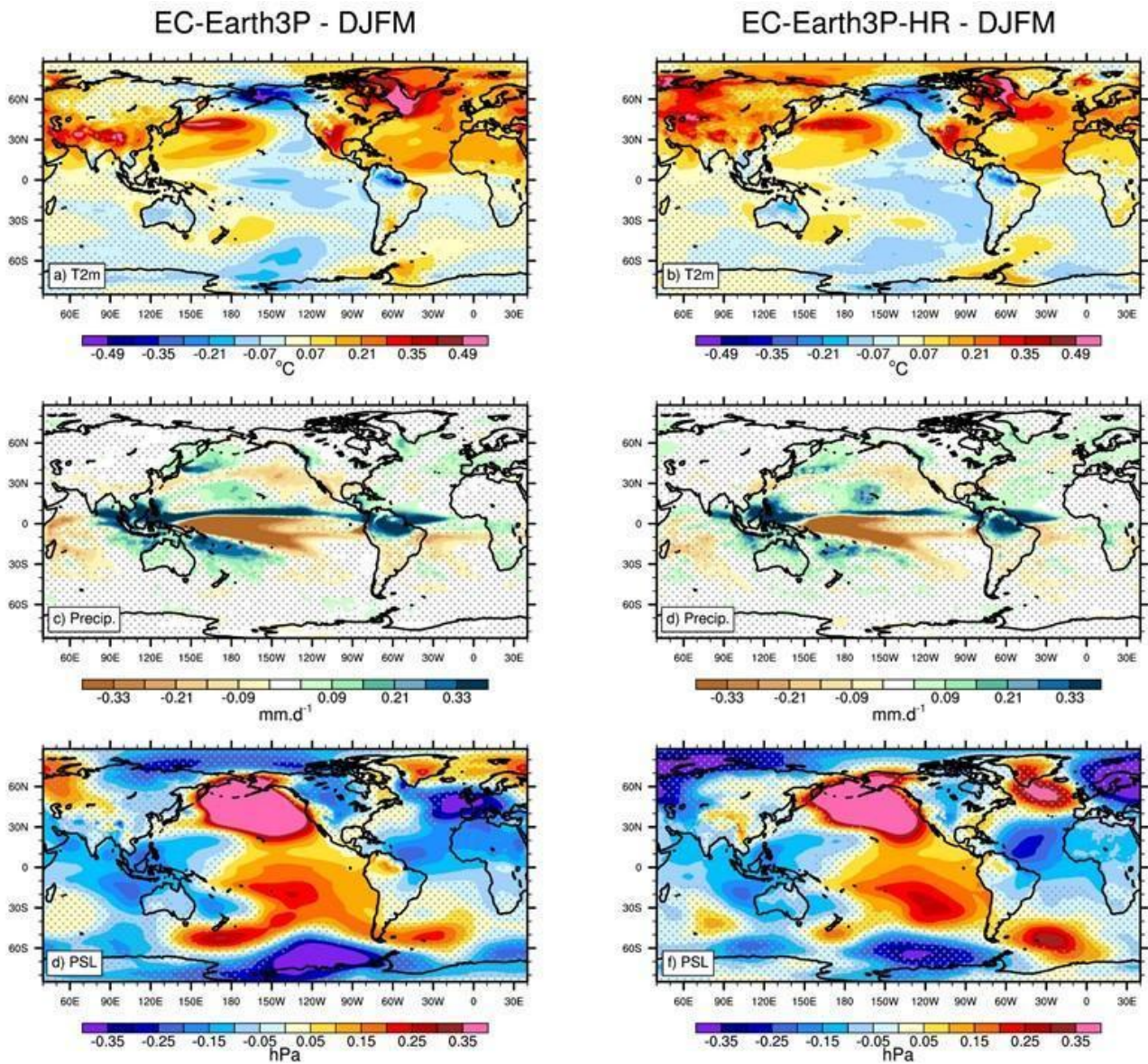


**Figure 2:** Differences between the 10-yr average of AMV+ and AMV- ensemble simulations for the DJFM season. (a), (b) 2-meter air temperature, (c), (d) precipitation, and (e), (f) sea level pressure. Results from (left) EC-Earth3 and (right) EC-Earth3P-HR are shown. Stippling indicates regions that are below the 95% confidence level of statistical significance according to a two-sided Student's t test.

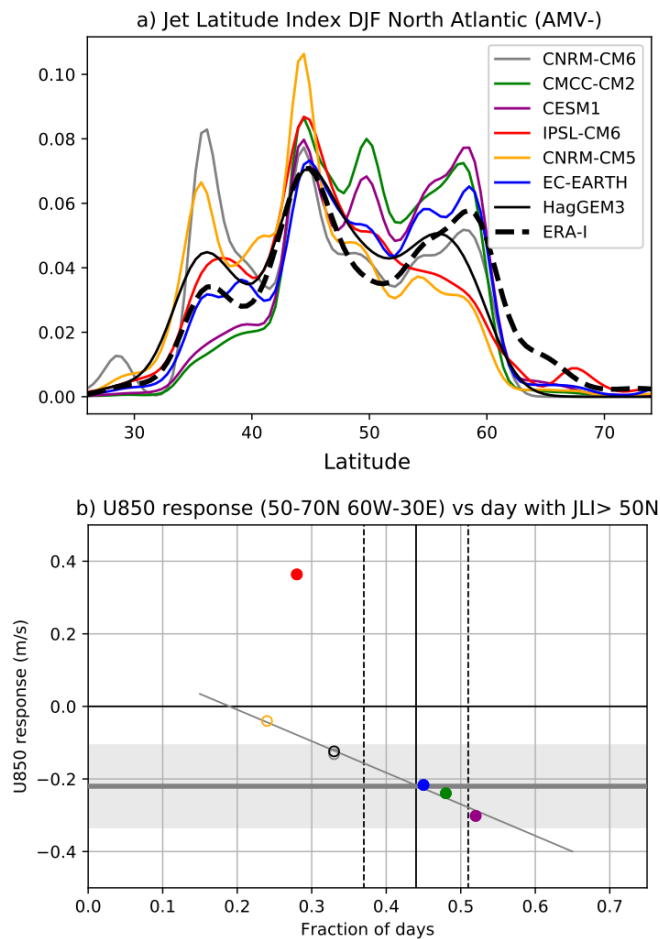


**Figure 3:** (a) Smooth density of the Jet Latitude Index (JLI) for AMV- experiments (solid lines) and ERA-Interim (bold dashed line) in DJF over the North Atlantic ( $30^{\circ}\text{W}-0^{\circ} / 15^{\circ}\text{N}-17^{\circ}\text{N}$ ). The JLI is defined as the latitude where the jet is maximum over a time running window of 10 days. (b) Relationship between the response of the zonal wind at 850 hPa averaged in the sector  $60^{\circ}\text{W}-30^{\circ}\text{E} / 50^{\circ}\text{N}-70^{\circ}\text{N}$  and the fraction of days with  $\text{JLI} > 50^{\circ}\text{N}$  in AMV-. A vertical solid line indicates the x value of ERA-Interim. Two dashed vertical lines mark the interval corresponding to one interannual standard deviation in ERA-Interim computed after a 10-yr running mean. Horizontal solid line marks the zero line. A bold, gray horizontal line indicates the value of the multimodel wind response. The shading indicates the confidence interval of the multimodel response. The thin gray line is a linear fit excluding the model with positive response (IPSL-CM6). Models with (without) a statistically significant response of the wind are indicated with a filled (empty) marker. From Ruggieri et al. (2021).

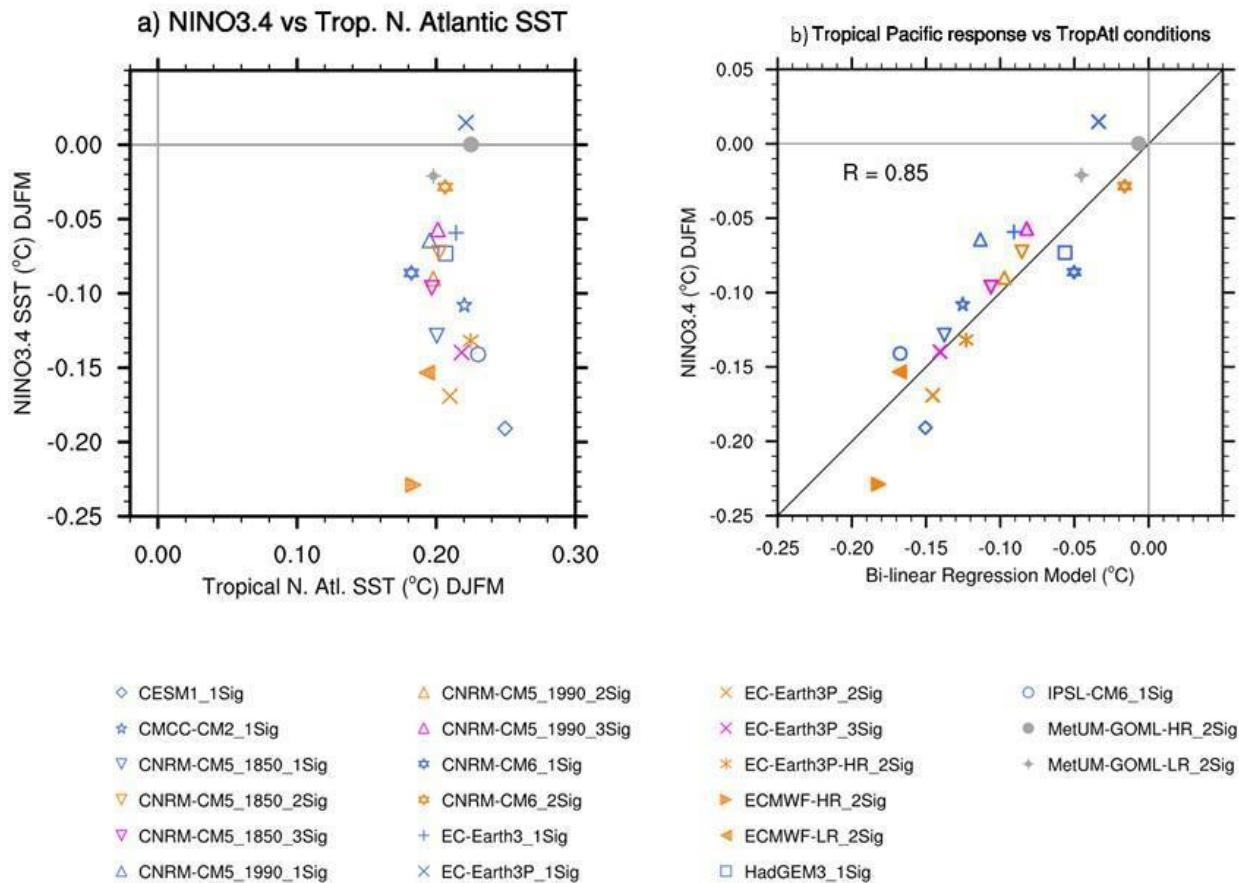


**Figure 4:** (a) Inter-model relationship between the winter (DJFM) NIÑO3.4 SST index versus winter tropical North Atlantic SST (averaged over 5°N-20°N / 60°W-10°E). Markers represent the 10-year averaged ensemble mean difference between AM+ and AMV- simulation from individual experiments. (b) Inter-model relationship between the winter (DJFM) NIÑO3.4 SST index versus a bi-linear regression model using the mean precipitation conditions over the East tropical Pacific and the tropical Atlantic during summer (JJAS) as predictors. From Ruprich-Robert et al. (2021).



## Part 2 - Seasonal Forecasts at High Resolution

The second part of the project aims to analyse the impact of increased resolution on seasonal forecast skill. Increasing the resolution of climate models, using in particular eddy-permitting configuration in the ocean, is a promising avenue to improve the predictive skill of our forecast systems. We expect to improve the representation of key teleconnection mechanisms, by enabling previously unresolved interactions of ocean eddies with the atmosphere (Mahajan et al., 2018), which in turn could increase the predictive skill of the systems, in particular over land.

We used the latest version of the coupled model EC-Earth3.3 (Döscher et al., 2021) in its high-resolution (HR) configuration (Haarsma et al., 2020). An important effort has been first dedicated to the tuning of this coupled configuration, to reduce the model biases and improve process-representation in the North Atlantic, a key region for decadal prediction skill. This tuning exercise has been performed on the BSC supercomputer and has involved the production of more than 15 different experiments and more than 1600 simulation years, which allowed us to define an optimal set of tuning parameters. One particularly interesting feature of this HR model version is the improvement in the simulated variability of the deep convection in the Labrador Sea and the Atlantic Meridional Overturning Circulation (AMOC) compared to the standard resolution (SR, of approximately 100 km in both the atmosphere and the ocean) version, which occurred too intermittently due to an overly strong local density stratification in this latter version. The decadal prediction system based on EC-Earth3.3-SR has been shown to experience a consistent collapse of the Labrador Sea convection (Bilbao et al, 2021). This collapse is caused by an initialization shock and induces a quick degradation of the predictive skill in the Subpolar North Atlantic, a source region of decadal variability and predictability (Smith et al, 2020). This problem is not present in EC-Earth3.3-HR, for which the Labrador Sea convection remains active and stable, positively impacting the strength of the AMOC (see Figure 5).

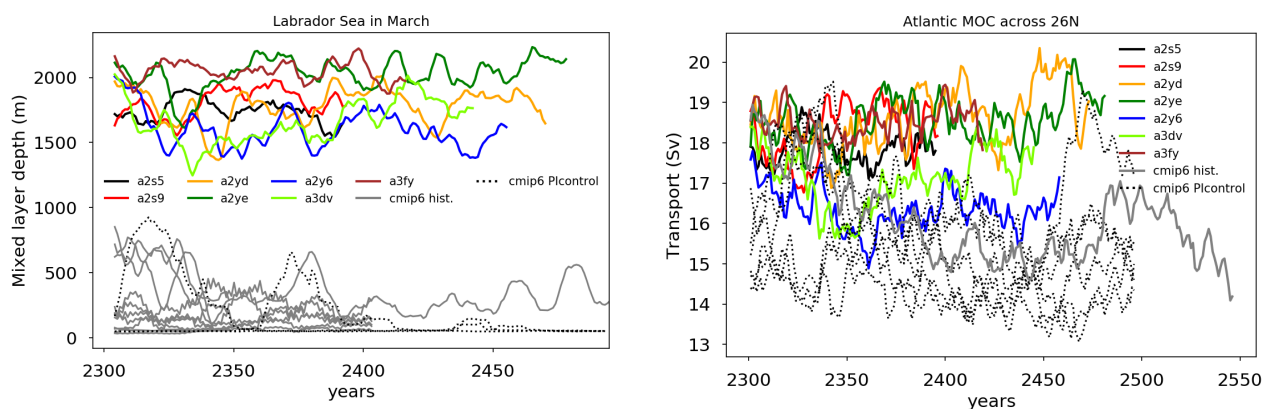


**Figure 5:** (left) Time-series of the mixed layer depth in the Labrador Sea in March for the different high-resolution experiments with a fixed forcing of the year 1980 (colored lines) compared to the standard-resolution experiments with a fixed forcing of the pre-industrial period (black dashed lines) and with the historical forcing (1850-2014) (grey lines). The mixed layer depth is a proxy of the deep convection of mass waters. (right) Time-series of the AMOC for the same experiments (only one standard resolution experiment with historical forcing - grey line). The decrease in the formation of deep water masses translates into a stronger AMOC, much closer to the observed values at 26°N of ~18 Sv. The y-axis corresponds to simulated (non-calendar) years.

Additional improvements of the seasonal forecast system have been made by enhancing the initialization procedure. We have developed a new refined strategy to improve the in-house reconstructions used to initialise our forecast systems. The goal was to find a method to assimilate ORAS5 temperature and salinity information (a reanalysis product of particular interest for having the same resolution as the HR version as EC-Earth), while preventing the inclusion of the non-stationary long-term biases in the western North Atlantic that have been documented for that product (Tietsche et al 2020). The tests included using nudging coefficients of different strength, disabling the nudging at specific regions and/or depths, and combining ORAS5 with other products. The best strategy was selected by performing a series of reduced seasonal prediction systems, each one initialised from one of the tested reconstructions, and computing the associated skill. The best performing approach resulted from combining the assimilation of two datasets, sea temperature and salinity at the surface from the ORAS5 ocean reanalysis and 3D ocean temperature and salinity below the mixed layer from the EN4 ocean reanalysis.

In a subsequent step we produced a retrospective seasonal forecast system with the tuned version of the coupled model, whose oceanic and sea-ice initial conditions come from the new in-house HR reconstruction, which follows the best strategy previously identified at low resolution. The atmospheric initial conditions of the seasonal forecast were taken from the ERA5 reanalysis and interpolated to the same grid of the HR version of IFS, the atmospheric component of EC-Earth. The initial conditions of the ocean and sea ice come from the in-house HR ocean-sea ice forced simulation described previously, with NEMO3.6-LIM3 (the corresponding ocean-sea ice components of EC-Earth), driven by ERA5 atmospheric fluxes and assimilating ORAS5 and EN4 ocean reanalysis. The ensemble of initial conditions has been generated by introducing random perturbations in the temperature fields of the interpolated atmospheric initial conditions.

We produced a retrospective seasonal forecast including 14 members, each of them initialised in the 1st of May and with a forecast range of 8-months to cover the following fall and early winter. The different forecasts have been initialised each year from 1990 to 2015. We modified the setup of the seasonal forecast system as we have decided to focus on a system initialized in May to investigate the typical rather stable skill conditions for ENSO predictability from summer through winter (Exarchou et al., 2021). In particular, with respect to the original plan, we slightly decreased the hindcast period (1990-2015 versus 1980-2018) but increased the number of members (14 versus 10, to improve the identification of the predictable signals) as well as the number of forecasted months (8 versus 6, to cover until December months). This modification of the setup was made possible by the drastic improvement in performance that we were able to obtain, after performing a thorough load balance analysis to optimise energy to solution on the ECMWF machine. While at the time of the proposal we estimated a consumption of 336,000 SBU per year, we have now reached an improved performance of 268,000 SBU per year. This configuration leads to a total of equivalent years of 243 years.

The analyses of the results show in particular increased predictive skill of El Niño-Southern Oscillation (ENSO) of this seasonal forecast system compared to the equivalent seasonal forecast but at standard resolution (SR), and also better skill when compared to the operational forecast of ECMWF, SEAS5 (Figure 1, left). The new forecast system also showed greatly improved skill in the Labrador Sea region where the non-stationary bias of ORAS5 had been shown in Tietsche et al (2020) to quickly degrade the predictive skill in SEAS5 (Figure 6, right).

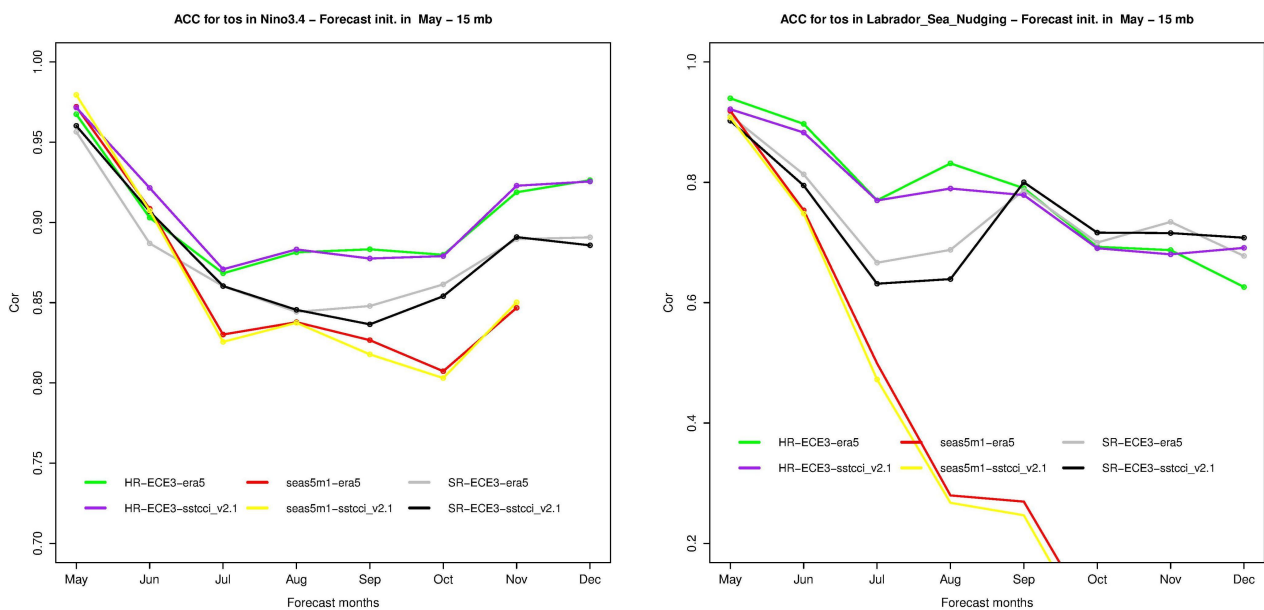


**Figure 6:** Anomaly correlation coefficients at each forecast month (May to December) of the surface sea temperature in (left) Niño3.4 region (5N-5S, 170W-120W) and (right) Labrador Sea region (50-65N, 60-35W) for the HR seasonal forecast compared to the ERA5 reanalysis (green line) and to the ESA SST CCI observational product (purple line), the equivalent SR seasonal forecast (grey and black lines respectively) and the ECMWF operational seasonal forecast SEAS5 (red and yellow lines respectively). All predictions are initialised on the 1st of May, have an ensemble size of 14 members and cover the reforecast period 1990-2015.

## References

Bilbao, R., S. Wild, P. Ortega, J. Acosta-Navarro, T. Arsouze, P.-A. Bretonnière, L.-P. Caron, M. Castrillo, R. Cruz-García, I. Cvijanovic, F.J. Doblas-Reyes, M. Donat, E. Dutra, P. Echevarría, A.-C. Ho, S. Loosveldt-Tomas, E. Moreno-Chamarro, N. Pérez-Zanon, A. Ramos, Y. Ruprich-Robert, V. Sicardi, E. Tourigny and J. Vegas-Regidor (2021). Assessment of a full-field initialised decadal climate prediction system with the CMIP6 version of EC-Earth. *Earth System Dynamics*, 12, 173-196, doi:10.5194/esd-2020-66.

Boer, G. J., Smith, D. M., Cassou, C., Doblas-Reyes, F., Danabasoglu, G., Kirtman, B., Kushnir, Y., Kimoto, M., Meehl, G. A., Msadek, R., Mueller, W. A., Taylor, K. E., Zwiers, F., Rixen, M., Ruprich-Robert, Y., and Eade, R. (2016) The Decadal Climate Prediction Project (DCPP) contribution to CMIP6, *Geosci. Model Dev.*, 9, 3751–3777, <https://doi.org/10.5194/gmd-9-3751-2016>.

Dong, B., Sutton, R. T., and Scaife, A. A. (2006), Multidecadal modulation of El Niño–Southern Oscillation (ENSO) variance by Atlantic Ocean sea surface temperatures, *Geophys. Res. Lett.*, 33, L08705, doi:[10.1029/2006GL025766](https://doi.org/10.1029/2006GL025766).

Döscher, R., Acosta, M., Alessandri, A., Anthoni, P., Arsouze, T., Bergman, T., Bernardello, R., Boussetta, S., Caron, L.-P., Carver, G., Castrillo, M., Catalano, F., Cvijanovic, I., Davini, P., Dekker, E., Doblas-Reyes, F. J., Docquier, D., Echevarria, P., Fladrich, U., Fuentes-Franco, R., Gröger, M., v. Hardenberg, J., Hieronymus, J., Karami, M. P., Keskinen, J.-P., Koenigk, T., Makkonen, R., Massonnet, F., Ménégos, M., Miller, P. A., Moreno-Chamarro, E., Nieradzki, L., van Noije, T., Nolan, P., O'Donnell, D., Ollinaho, P., van den Oord, G., Ortega, P., Prims, O. T., Ramos, A., Reerink, T., Rousset, C., Ruprich-Robert, Y., Le Sager, P., Schmith, T., Schrödner, R., Serva, F., Sicardi, V., Sloth Madsen, M., Smith, B., Tian, T., Tourigny, E., Uotila, P., Vancoppenolle, M., Wang, S., Wårlind, D., Willén, U., Wyser, K., Yang, S., Yepes-Arbós, X., and Zhang, Q. (2022) The EC-Earth3 Earth system model for the Coupled Model Intercomparison Project 6, *Geosci. Model Dev.*, 15, 2973–3020, <https://doi.org/10.5194/gmd-15-2973-2022>.

Haarsma, R., M. Acosta, R. Bakhshi, P.-A. Bretonnière, L.-P. Caron, M. Castrillo, S. Corti, P. Davini, E. Exarchou, F. Fabiano, U. Fladrich, R. Fuentes Franco, J. García-Serrano, J. von Hardenberg, T. Koenigk, X. Levine, V. Meccia, T. van Noije, G. van den Oord, F.M. Palmeiro, M. Rodrigo, Y. Ruprich-Robert, P. Le Sager, E. Tourigny, S. Wang, M. van Weele and K. Wyser (2020). HighResMIP versions of EC-Earth: EC-Earth3P and EC-Earth3P-HR. Description, model performance, data handling and validation. *Geoscientific Model Development*, 13, 3507-3527, doi:10.5194/gmd-2019-350.

Ishii, M., M. Kimoto, K. Sakamoto, and S. Iwasaki (2005) Subsurface Temperature And Salinity Analyses. Research Data Archive at the National Center for Atmospheric Research, Computational and Information Systems Laboratory. <https://doi.org/10.5065/Y6CR-KW66>.

Ruprich-Robert, Y., Msadek, R., Castruccio, F., Yeager, S., Delworth, T., & Danabasoglu, G. (2017). Assessing the Climate Impacts of the Observed Atlantic Multidecadal Variability Using the GFDL CM2.1 and NCAR CESM1 Global Coupled Models, *Journal of Climate*, 30(8), 2785-2810, doi:[10.1175/JCLI-D-16-0127.1](https://doi.org/10.1175/JCLI-D-16-0127.1)

Ruprich-Robert, Y., Delworth, T., Msadek, R., Castruccio, F., Yeager, S., & Danabasoglu, G. (2018). Impacts of the Atlantic Multidecadal Variability on North American Summer Climate and Heat Waves, *Journal of Climate*, 31(9), 3679-3700, doi:[10.1175/JCLI-D-17-0270.1](https://doi.org/10.1175/JCLI-D-17-0270.1)

Tietsche, S., M. Balmaseda, H. Zuo, C. Roberts, M. Mayer and L. Ferranti (2020) The importance of North Atlantic Ocean transports for seasonal forecasts. *Clim Dyn* 55, 1995–2011. <https://doi.org/10.1007/s00382-020-05364-6>

Zanchettin, D., Bothe, O., Graf, H. F., Omrani, N.-E., Rubino, A., and Jungclaus, J. H. (2016), A decadal delayed response of the tropical Pacific to Atlantic multidecadal variability, *Geophys. Res. Lett.*, 43, 784– 792, doi:[10.1002/2015GL067284](https://doi.org/10.1002/2015GL067284).

Zhang, R., and Delworth, T. L. (2006), Impact of Atlantic multidecadal oscillations on India/Sahel rainfall and Atlantic hurricanes, *Geophys. Res. Lett.*, 33, L17712, doi:10.1029/2006GL026267.

## List of publications/reports from the project with complete references

Ruggieri, P., Bellucci, A., Nicolí, D., Athanasiadis, P. J., Gualdi, S., Cassou, C., Castruccio, F., Danabasoglu, G., Davini, P., Dunstone, N., Eade, R., Gastineau, G., Harvey, B., Hermanson, L., Qasmi, S., Ruprich-Robert, Y., Sanchez-Gomez, E., Smith, D., Wild, S., & Zampieri, M. (2021). Atlantic Multidecadal Variability and North Atlantic Jet: A Multimodel View from the Decadal Climate Prediction Project, *Journal of Climate*, 34(1), 347-360, doi:[10.1175/JCLI-D-19-0981.1](https://doi.org/10.1175/JCLI-D-19-0981.1)

Ruprich-Robert, Y., E. Moreno-Chamarro, X. Levine, A. Bellucci, C. Cassou, F. Castruccio, P. Davini, R. Eade, G. Gastineau, L. Hermanson, D. Hodson, K. Lohmann, J. Lopez-Parages, P.-A. Monerie, D. Nicoli, S. Qasmi, C. D. Roberts, E. Sanchez-Gomez, G. Danabasoglu, N. Dunstone, M. Martin-Rey, R. Msadek, J. Robson, D. Smith and E. Tourigny (2021). Impacts of Atlantic Multidecadal Variability on the Tropical Pacific: a multi-model study. *npj Climate and Atmospheric Science*, 4, 33, doi:10.1038/s41612-021-00188-5.

European Climate Prediction system (EUCP) HORIZON 2020 project, THEME SC5-2017 - Deliverable 1.3 “Recommendations for the development of a new generation of climate forecast systems.”

## Future plans

A continuation of this Special Project is underway with the Special Project granted for 2022 entitled “High-resolution ocean reconstructions for initializing decadal climate predictions”, which will enable us to have more realistic initial conditions for the ocean and sea-ice for a reduced set up of HR decadal prediction systems, which is another challenge from a computing resource perspective.